HHS Public Access

Author manuscript

*Acta Biomater*. Author manuscript; available in PMC 2019 September 01.

Published in final edited form as:

*Acta Biomater*. 2018 September 01; 77: 116–126. doi:10.1016/j.actbio.2018.07.009.

# Development of an Apoptosis-Assisted Decellularization Method for Maximal Preservation of Nerve Tissue Structure: Apoptosis-Assisted Decellularization for Maximal Nerve Tissue Preservation

**R.C. Cornelison**[1,2], **S.M. Wellman**[2], **J.H. Park**[2], **S.L. Porvasnik**[2], **Y.H. Song**[2], **R.A. Wachs**[2,*], and **C.E. Schmidt**[2,*]

[1]McKetta Department of Chemical Engineering, University of Texas at Austin, Austin, TX 78705

[2]J. Crayton Pruitt Department of Biomedical Engineering, University of Florida, Gainesville, FL 32611

## Abstract

Preservation of tissue structure is often a primary goal when optimizing tissue and organ decellularization methods. Many current protocols nonetheless rely on detergents that aid extraction of cellular components but also damage tissue architecture. It may be more beneficial to leverage an innate cellular process such as apoptosis and promote cell removal without the use of damaging reagents. During apoptosis, a cell detaches from the extracellular matrix, degrades its internal components, and fragments its contents for easier clearance. We have developed a method that leverages this process to achieve tissue decellularization using only mild wash buffers. We have demonstrated that treating peripheral nerve tissue with camptothecin induced both an early marker of apoptosis, cleaved caspase-3 expression, as well as a late stage marker, $TUNEL^+$ DNA fragmentation. Clearance of the cellular components was then achieved in an apoptosis-dependent manner using a gentle wash in hypertonic phosphate buffered saline followed by DNase treatment. This wash paradigm did not significantly affect collagen or glycosaminoglycan content, but it was sufficient to remove any trace of the cytotoxic compound based on conditioned media experiments. The resulting acellular tissue graft was immunogenically tolerated *in vivo* and exhibited an intact basal lamina microarchitecture mimicking that of native, unprocessed nerve. Hence, *ex vivo* induction of apoptosis is a promising method to decellularize tissue without the use of harsh reagents while better preserving the benefits of native tissue such as tissue-specific composition and microarchitecture.

[*]Co-corresponding authors: schmidt@bme.ufl.edu, Ph (352)273-9222, F (352)273-9221, rebecca.wachs@unl.edu, Ph (402)472-2262, F (402)472-6338.

[#]Current address for RAW is 248 L. W. Chase Hall, Department of Biological Systems Engineering, University of Nebraska, P.O. Box 830726, Lincoln, NE 68583-0726, BMSB JG-42 P.O. Box 116131 Gainesville, FL 32611

7. Disclosures

The authors report no financial conflicts of interest regarding this work.

**Keywords**

Decellularization; detergent-free; apoptosis; peripheral nerve graft

## 1. Introduction

Tissue-based scaffolds hold significant promise for tissue and organ regeneration. The internal structure can be a critical factor in the success of the scaffold, particularly for peripheral nerve regeneration [1–3]. For example, nerve grafts with aligned structures promote directionality and increase the speed of axon growth compared to grafts devoid of structure [4]. Hence, a nerve autograft is the gold standard for peripheral nerve repair in humans: A piece of existing nerve tissue containing native channel structures is harvested from the patient and implanted at the injury site. Nevertheless, nerve autografting requires a separate surgery for tissue harvest and results in loss of function at the harvest site. To eliminate these drawbacks, several protocols have been developed to render allogeneic nerve tissue non-immunogenic through the process of decellularization [5–9].

The vast majority of decellularization protocols start with an incubation step in water – a hypotonic solution that lyses resident cells and disperses antigenic cellular remnants throughout the tissue [10]. These remnants must then be removed to avoid deleterious immune reactions, often through harsh chemicals such as detergents [11–13]. These processing conditions are unfortunately known to remove desired extracellular matrix components, induce tissue swelling, and damage the native tissue structure [8,14]. Therefore, excluding these harsh conditions has the potential to enhance structural preservation and functionality of the resulting tissue graft. We sought to create an alternative decellularization protocol capitalizing on the innate process of programmed cell death or apoptosis. Through apoptosis, cells detach from the extracellular matrix, degrade their proteins and nucleic acids, and sequester their contents into small fragments. Therefore, induction of apoptosis is an ideal method for the generation of intact, acellular tissue.

We show that treating isolated nerve tissue with the small molecule cytotoxin camptothecin induces apoptosis and facilitates elimination of antigenic cellular components without requiring cell lysis buffers or harsh chemicals. Camptothecin treatment increased early and late stage markers of apoptosis in *ex vivo* nerve tissue, and marker expression was dependent upon drug treatment. Furthermore, induction of apoptosis enabled removal of cellular components using a hypertonic buffer and DNase treatment instead of surfactants. The optimal decellularization protocol effectively preserved extracellular matrix components, such as collagen and glycosaminoglycans (GAGs), while removing approximately 95% of DNA. The apoptosis decellularized (AD) nerve grafts did not contain cytotoxic residual chemicals and were immunologically tolerated in a rat subcutaneous implant model. Most noteworthy, this novel method of apoptosis-assisted decellularization preserved the native nerve architecture far better than methods using water for cell lysis, and the structure of these processed tissue grafts was nearly identical to that of unprocessed peripheral nerve.

## 2. Materials and methods

### 2.1. Tissue harvest and apoptosis-assisted decellularization

All animal work was approved by the Institutional Animal Care and Use Committee at the University of Florida. Sciatic nerves were aseptically harvested from adult Sprague-Dawley (SD) rats. Tissues of approximately 1.5–2 cm long were collected by transecting the sciatic nerve distal to both the greater sciatic foramen and the sciatic trifurcation. Fatty and connective tissue was removed from the epineurium using fine forceps and a Leica Zoom 2000 microscope, and the nerve tissue was transferred to a sterile 15 mL conical tube. Tissue processing was initiated by adding serum-free DMEM-F12 (Gibco, Waltham, MA) with or without camptothecin (Sigma, Carlsbad, CA) at either 5 or 10 μM, a common concentration range used in the literature [15,16]. The tissue was placed on a vertical tube revolver (Thermo Scientific) at 14 rpm and 37°C for 1, 2, or 3 days. The tissue was then either processed for immunohistochemistry to examine the extent of tissue-wide apoptosis or subjected to various wash buffers, as described below. As a standard for comparison, detergent-decellularized nerve grafts were also generated using the detergent decellularization (DD) method previously described by Hudson et al. [8].

### 2.2. Verification of apoptosis induction

The ability to induce apoptosis in *ex vivo* tissue was evaluated using immunohistochemistry and two markers of apoptosis, one early-stage and one late-stage marker. Active caspase-3 was used as an early marker of apoptosis [17], and DNA fragmentation was used as a latestage marker, identified using terminal dUTP nick-end labeling (TUNEL) [18]. Nerve tissue was fixed in 4% paraformaldehyde for 1 hour at room temperature, washed with 1X PBS, and processed for cryosectioning. The tissue was cryopreserved by incubating in 30% sucrose for 3 days, embedded in Optimum Cutting Temperature medium (OCT, Sakura Finetek; Torrance, CA), frozen, and cut into 12 μM sections using a CM1950 Leica cryostat.

Induction and extent of early-stage apoptosis was evaluated using a rabbit antibody against caspase-3 used at 1:200 (ab13847, Abcam; Cambridge, UK). Some sections were also stained against heavy chain neurofilaments (1:500) to assess co-localization with neuronal processes (RT-97; Developmental Hybridoma Studies Bank, Iowa City, IA). Tissue sections were blocked for 1 hour at room temperature in 3% goat serum and 0.3% Triton X-100 in 1X PBS. The primary antibodies was then diluted in the blocking buffer and incubated on the tissue overnight at 4°C. After washing three times in 1X PBS for 5 minutes each, anti-rabbit Alexa Fluor 594 was diluted in blocking buffer (1:500) and incubated for 1 hour at room temperature in the dark. Antimouse Alexa Fluor 488 was also added when necessary for neurofilament staining. The tissue was again washed with 1X PBS, and nuclei were counterstained with DAPI (Thermo Fisher Scientific, Waltham, MA). Samples were mounted with Fluoromount-G (Southern Biotech, Birmingham, AL) and coverslipped. Immunohistochemistry was performed on a minimum of three nerves over multiple rounds of decellularization and evaluated at three locations 120 μm apart.

Adjacent tissue sections were also assessed for late-stage DNA damage using a fluorescence TUNEL kit according to manufacturer's instructions (Roche, Basel, SUI) [19]. Briefly,

frozen sections were encircled using a hydrophobic SecureSeal imaging Spacer (Grace Biolabs; Bend, OR) and incubated with 50 μL of Proteinase K solution at 0.61 U/mL for 15 minutes. The sections were washed two times in deionized water for two minutes each. Samples were then treated with 1X TdT labeling buffer for 10 minutes followed by incubation in 20 μL of reaction mix (containing biotin-16-dUTP, 5 mM $CoCl_2$, and TdT enzyme) in a humidified chamber for 60 minutes. The TdT enzyme was omitted to generate a negative control, and sections were treated with 10,000 U/mL DNase for a positive control. After stopping the reaction using 4 μL of 0.1 M EDTA, samples were incubated with streptavidin Alexa Fluor 488 for 20 minutes in the dark, washed three times with 1X PBS, and counterstained using DAPI. Images were acquired using a Zeiss Axio Imager.Z2 microscope and Zen software (Oberkochen, DEU).

### 2.3. Wash parameter optimization

Several wash buffers and conditions were examined for achieving effective apoptotic body removal. The focus of buffer selection was on use of hypertonic and hypotonic conditions to eliminate the need for water washes and detergent solutions. After incubation with either blank medium control or medium containing camptothecin for apoptosis induction, the tissue was washed with mildly hypotonic 0.5X PBS, isotonic 1X PBS, or hypertonic 4X PBS on a vertical agitator at 14 rpm and room temperature for 6–24 hours. These buffers were also examined in tandem using first a hypertonic wash that was gradually graded into a hypotonic wash (refer to **Figure 3A**). Some samples were also treated with 75 U/mL DNase (Sigma) for 24 hours at room temperature followed by three 1 hour washes in 1X PBS. The effectiveness of various wash parameters was assessed using immunohistochemistry and DNA quantification.

### 2.4. Generation of apoptosis decellularized nerve

Except for DNase treatment, all of the following steps were performed on a vertical agitator at 14 rpm. Cleaned peripheral nerves were incubated in 15 mL of medium containing 5 μM camptothecin for 24 hours at 37°C. The tissue was then washed with hypertonic 4X PBS at room temperature for another 24 hours. The wash buffer was graded down to 2X PBS then 1X PBS, 30 minutes each, and the 1X PBS wash was repeated twice more (total of three times). The tissue was then incubated in 200 μL of 75 U/mL DNase for 36 hours at room temperature. After washing twice in 1X PBS for 30 minutes each, the tissue was stored in 1X PBS until use.

### 2.5. Examination of cell antigen removal and extracellular matrix component maintenance

The presence of residual cellular antigens was evaluated by labeling against neurofilament (1:500, RT-97, Developmental Hybridoma Studies Bank, Iowa City, IA) for neurons and S-100 protein (1:400, Z0311, Dako, Santa Clara, CA) for Schwann cells ($n \geq 3$). Tissue structure and preservation were assessed using an antibody against laminin (1:500, L9393, Sigma). Immunohistochemistry was performed as described in 2.2 above for caspase-3. Residual DNA was quantified using a Quant-iT™ PicoGreen™ dsDNA assay (Invitrogen), and collagen and sulfated GAG content were quantified using Sircol and Blyscan kits,

respectively (Biocolor, Ltd; Carrickfergus, UK). Each procedure was conducted according to the manufacturer's instructions. Unprocessed nerve samples were used as controls.

### 2.6. Assessment of cytotoxic residuals

Conditioned media were used to test for the presence of leachable residual drug or chemicals following *in vitro* decellularization processing [20]. Segments of unprocessed nerve, apoptosis decellularized (AD) nerve, or detergent-decellularized (DD) nerve were incubated in 3:1 DMEM:F12 medium for 72 hours at 37°C (one nerve in one mL of medium, n=5 per group). Adult rat Schwann cells were then seeded in either a 24-well plate at 30,000 cells per well or a 96 well plate at 3,500 cells per well. The following day, conditioned media were added to the Schwann cell cultures for 48 hours. The medium was then exchanged for medium containing alamarBlue Cell Viability Assay Reagent (Thermo) diluted 1:10, followed by incubation at 37˚C for 3 hours. For each sample well, 100 μL of medium was transferred into a clear 96 well plate, and absorbance was measured at 570/600 nm using a microplate reader (BioTek). Absorbance values were converted to percent metabolic reduction of alamarBlue according to manufacturer's instructions [21].

### 2.7. Subcutaneous implantation of nerve scaffolds

Forty-eight male Lewis rats (250–300g; Charles River Laboratories) were randomly divided into four experimental groups that were evaluated at three time points post-implantation (n=4 per group per time point at 1, 2, and 4 weeks): 1) AD scaffold, 2) DD scaffold, 3) unprocessed Sprague Dawley nerve (allograft positive control), and 4) unprocessed Lewis nerve (isograft negative control). Animals were anesthetized and maintained on 1.5–2% isoflurane/oxygen for the duration of the procedure using aseptic techniques. A subcutaneous pocket was made through a skin incision starting over the vastus lateralis muscle extending caudally 1 cm. A single 4 mm piece of one of the four experimental tissue groups was implanted into the subcutaneous pocket. The incision was closed using 5–0 PGCL (AD Surgical, CA) in a subcuticular suture pattern. Animals received loxicom (1 mg/kg; Patterson Veterinary) for 48 hours after surgery for pain management. After 1, 2 and 4 weeks post-implantation, the animals were euthanized and the implanted tissue samples were harvested, embedded, and sectioned in preparation for histology.

### 2.8. Histopathology and immunohistochemistry

Histological examinations of the scaffolds and nerve tissue were performed using hematoxylin and eosin (H&E) stained frozen sections imaged on a Zeiss Axio Observer.Z1 microscope (Zeiss, Micro Optics of Florida, Inc.) (n=4 per group per time point, except n=1 for DD at 4 weeks). The pathological changes of implanted tissues were evaluated for inflammatory cell infiltrate and stromal cell remodeling. Inflammatory infiltration (e.g., macrophages, polymorphonuclear cells, eosinophils, and mast cells) was identified based on the presence of small, round cells with dark purple nuclear staining. Stromal remodeling was defined as a mixture of migrating cells, fibroblasts or Schwann cells for example, that take up residence in the scaffold and was identified based on an elongated morphology that extended beyond the purple nuclear staining. In each experimental group, five serial tissue sections (10 μm each) were placed on each slide so that every slice was 50 μm apart and the first and last sections were scored for pathological changes in five different fields of view

(FOV) at 40X magnification using two visual center fields and three visual fields at the edge of the tissue. A five-step scoring system was designed with the help of a pathologist to evaluate histopathological remodeling in each group. The scores were based on the percent of area coverage in the FOV: 0 = no changes (0% FOV); 1= minimal changes (<25% FOV); 2 = mild changes (25–50% FOV); 3 = moderate changes (51–75% FOV); 4 = severe changes (>75% FOV); 5 = completely remodeled (100% FOV). Examples of each score are shown in **Supplemental Table 1**. Each section was scored twice at different times by the same observer, once blinded for both the group and time point then once blinded by group only. Representative images of H&E sections were taken at 5X and 40X using an Olympus BX43 microscope and DP80 camera (Hunt Optics & Imaging) using cellSens software (Olympus).

Macrophage infiltration was assessed via immunofluorescence staining for CD68 (MCA341R, Abd Serotec) [22]. Images were acquired using a Zeiss Axio Imager Z2 microscope (Zeiss, Micro Optics of Florida, Inc.). Four images were evaluated for each sample at each time point, and a set area was selected in the center of each image field for quantification. The intensity sum of the $CD68^+$ macrophages was quantified using ZEN Pro microscopy software (Zeiss) and normalized to total image area for each sample. Data from the four images were averaged to obtain a representation of a single animal. The presented data are an average of each animal per group per time point (n=4 per group per time point, except n=1 for DD at 4 weeks).

### 2.9. Statistics

Analysis of Variance (ANOVA) was used to determine if statistical significance was present among groups of three or more. If significance was found, Dunn's multiple comparisons test was performed using a significance level of $\alpha$=0.05. For collagen and GAG quantification, unpaired student's t-tests were used to compare unprocessed and AD nerve samples. All data are presented as mean ± standard error of the mean.

## 3. Results

### 3.1. Camptothecin induces wide-spread apoptosis in *ex vivo* tissue

It was first verified that apoptosis could be induced in *ex vivo* tissue and was dependent on drug treatment. Unprocessed nerve tissue displayed no signs of early or late-stage apoptosis (**Figure 1A, E**) nor did tissue maintained in serum-free medium at 37°C for up to 2 days (**Figure 1B, F**). Conversely, treating nerve tissue with 5–10 μM camptothecin for at least one day *in vitro* resulted in extensive immunoreactivity for the early stage apoptosis marker cleaved caspase-3 after one day (**Figure 1C, D-G**). Furthermore, DNA strand breaks – a late stage marker of apoptosis [18] – were identified by terminal dUTP end-nick labeling (TUNEL) in camptothecintreated tissue (**Figure 1G, H**). Camptothecin is known to activate the intrinsic apoptosis pathway, requiring a nucleus [23], yet peripheral nerve cell bodies primarily reside in the dorsal root ganglia adjacent to the spinal cord. We therefore qualitatively assessed if apoptosis was occurring in neuronal projections in addition to non-neuronal cells such as Schwann cells and fibroblast. Neurofilament staining appeared to co-localize with cleaved caspase-3 staining, indicating induction of caspase-3 activation in axons even in the absence of neuronal soma (**Figure 1I-K**).

### 3.2. Induction of apoptosis facilitates cellular antigen removal

After confirming the presence of apoptotic markers, we evaluated the potential to remove the prospective cell fragments resulting from apoptosis without the use of detergents. The agitation used during camptothecin treatment alone was not sufficient to remove many cellular proteins (**Supplemental Figure 1A**), nor was washing with isotonic 1X PBS for up to 24 hours (data not shown). In an effort to avoid the use of water and detergent solutions, we examined the use of two non-isotonic buffers: hypertonic 4X PBS and mildly hypotonic 0.5X PBS. The tissue was first treated with 5 μM camptothecin for 2 days, then washed overnight with the respective buffer. Overnight washes of hypertonic solutions achieved better protein removal (**Supplemental Figure 1B**) whereas hypotonic solutions removed more nuclei (**Supplemental Figure 1C**). The combination of hypertonic and hypotonic washes, in that order, provided the benefits of both methods for wash durations of 24 hours and 18 hours, respectively.

We then used this combination wash strategy to qualitatively assessed antigen removal as a function of both camptothecin concentration (5 and 10 μM) and treatment duration (1 and 2 days *in vitro*). Unprocessed nerve samples showed ample cellular antigens throughout the tissue (**Figure 2A**). Without camptothecin treatment to induce apoptosis, the combinatorial wash strategy had no apparent effect on protein or DAPI immunoreactivity (**Figure 2B**). Conversely, washing after treating with 5 μM camptothecin for one day (**Figure 2C**) observably decreased the immunoreactivity more than treating for longer or with more concentrated doses (**Figure 2D and 2E**, respectively). These results were in contrast to our previous evidence that increasing drug duration and concentration increased apoptotic marker expression, indicating the ease of antigen removal using this combination hypertonic-hypotonic wash strategy did not linearly correlate with the extent of apoptosis.

It has been proposed that a decellularization process should remove >95% of DNA within a tissue to adequately prevent an immune reaction upon implantation [24]. Using the combination hypertonic-hypotonic wash strategy, all of the drug treatments tested significantly decreased DNA content compared to unprocessed nerve samples ($p<0.05$; $n=5$) (**Figure 2G**). Additionally, all of the conditions were significantly different from nerves processed using only the wash regimen, except the group treated with 5 μM for 2 days ($p>0.1$; $n=5$), suggesting apoptosis was again necessary for antigen removal via this combination wash strategy. Interestingly, nerves treated at 5 μM for 2 days showed significantly increased DNA retention compared to nerves treated for only 1 day ($p<0.05$; $n=5$). The same was true for 10 μM, although the effect was insignificant ($p>0.1$; $n=5$).

Although the hypertonic-hypotonic wash strategy did significantly decrease DNA content following apoptosis, DNA retention was still well above 5%. Therefore, an alternative to the hypertonic-hypotonic wash method was developed by replacing the hypotonic wash with incubation in the DNA-degrading enzyme DNase. Unsurprisingly, this new regimen again significantly reduced DNA content for all conditions compared to unprocessed nerve ($p<0.001$; $n=5$). For nerves treated with either 5 or 10 μM camptothecin for 1 day, this hypertonic-DNase wash strategy resulted in a 95% reduction in the average DNA content (**Figure 2G**). The 10 μM treatment showed marginally higher DNA removal, but the lower 5

μM dose used less cytotoxic drug to achieve an adequate outcome. Therefore, the optimal conditions of apoptosis decellularization were selected as 5 μM treatment for 1 day followed by a 24 hour, 4X PBS wash and 36 hour DNase treatment. The flow chart in **Figure 3A** details the processes tested, with the solid arrows and blue boxes showing the final process.

### 3.3. Apoptosis-assisted decellularization preserves matrix composition and structure

We assessed the ability of apoptosis decellularization to preserve desirable matrix components using commercially available quantitative assays. Total collagen content exhibited an apparent but insignificant increase following processing, from 8% (0.08 mg/mg) in unprocessed nerves to 12% (0.12 mg/mg) in apoptosis decellularized nerves (**Figure 3B**). Other matrix components such as glycosaminoglycans (GAGs) can also be beneficial for increasing growth factor binding upon implantation [25]. Apoptosis decellularization modestly, but insignificantly, decreased sulfated GAG content from 0.5 μg/mg in unprocessed nerves and 0.3 μg/mg in decellularized nerves (**Figure 3C**, $p>0.1$; $n=5$). Our previous work with detergent decellularization demonstrated an increased in nerve sulfated GAG content when normalizing to mass after processing, suggesting the hypertonic wash in apoptosis decellularization might remove more hydrophilic GAGs than do detergents. Nonetheless, apoptosis decellularization did not significantly alter the native collagen or sulfated GAG content by mass. In contrast, immunoreactivity for myelin-associated components like myelin basic protein visibly decreased following apoptosis decellularization (**Figure 3D-E**).

We also evaluated the structure of the nerve basal lamina pre-and post-apoptosis decellularization using immunohistochemistry. Apoptosis decellularized nerves demonstrated preservation of basal lamina similar to that in unprocessed nerves, as illustrated by laminin staining. (**Figure 3F and G**). Conversely, rinsing the nerve tissue in water, as is commonly done to induce cell lysis prior to decellularization, resulted in vast changes to the matrix structure (**Figure 3H**). The water wash did not qualitatively affect overall patency of the laminin channels but did increase the distance between the channels, indicative of tissue enlargement and decreased tissue integrity

### 3.4. Inducing tissue-wide apoptosis using camptothecin does not increase graft cytotoxicity

We assessed the possibility that the resulting nerve grafts would retain residual camptothecin that may contribute to graft-mediated cytotoxicity using conditioned media experiments. We compared four groups of conditioned medium: unprocessed nerve, apoptosis decellularized (AD) nerve, detergent-decellularized (DD) nerve, and pristine medium controls that were incubated without a tissue sample. Using reduction of alamarBlue as a metric for cellular activity, it was found that medium conditioned with AD nerve did not significantly alter Schwann cell metabolism compared to pristine controls, suggesting minimal cytotoxic residuals following decellularization (**Figure 4**). Conversely, medium conditioned with either unprocessed nerve or DD nerve significantly decreased Schwan cell reduction of alamarBlue. These effects may be explained by the release of stress-induced cytokines in the case of unprocessed nerves and by insufficient washing for DD nerves.

### 3.5. Apoptosis decellularized tissue is immunogenically tolerated *in vivo*

A subcutaneous implant model in Lewis rats was used to test the effectiveness of apoptosis decellularization for removing antigenic material and minimizing host immune response (**Figure 5**). AD nerves were compared to isograft negative controls (unprocessed Lewis nerves), allograft positive controls (unprocessed Sprague Dawley nerves), and DD nerves, which have previously been shown to be immunogenically tolerated in rats [26]. The nerve samples were well-maintained at the implant site, with each implant easily identifiable upon explant at weeks 1 and 2. Similar results were observed at week 4 except for the DD group, which had only one identifiable replicate remaining. These observations potentially indicate rapid degradation of DD nerves. The optimal half-life of a nerve graft has been suggested to be 3 weeks, with full degradation by 3 months [27,28]. While we did not determine the degradation rate of AD nerves, they at least were maintained beyond the optimal half-life period.

We used histopathology to compare inflammatory infiltration and stromal remodeling across the four groups (**Figures 5A-L**). Unprocessed Sprague Dawley nerves showed abundant cellular infiltrate in the implants while unprocessed Lewis nerves had a low degree of infiltration, establishing the upper and lower bounds of the inflammatory response. AD nerves exhibited minimal acute inflammatory reaction, with significantly less inflammatory infiltration at weeks 2 and 4 compared to allograft positive controls (**Figure 5M**) ($p<0.01$ and $p<0.001$, respectively; $n=4$). By week 4, inflammatory infiltration in AD nerves was significantly lower than the isograft negative controls ($p<0.05$; $n=4$ for AD group and $n=3$ for fresh Sprague Dawley group). Samples in the DD group exhibited wide variability in infiltration but were generally well tolerated by week two.

A stromal reaction to the implants, whether scaffolds or unprocessed tissue controls, was observed comprising fibroblasts, Schwann cells, and collagen (**Figure 5**). A strong stromal remodeling reaction was seen immediately at week 1 in the DD scaffold group (**Figure 5B**) that was significantly greater than the AD scaffold group (**Figure 5A**, $p<0.01$; $n=4$). The AD group had significantly less stroma at week 2 compared to the other groups (**Figure 5E**, $p<0.05$; $n=4$). At 4 weeks, the AD scaffold (**Figure 5I**) could still be seen and had not been completely remodeled with stromal tissue as was observed in the DD scaffold and unprocessed Lewis and SD controls (**Figures 5J-L**, respectively).

We next specifically examined macrophage infiltration using $CD68^+$ macrophage area coverage as an approximate measurement of the number or size (i.e., large, phagocytic) of macrophages [29]. Macrophage infiltration is beneficial early after peripheral nerve injury as it promotes debris clearance, but a pronounced and prolonged response by phagocytic, $CD68^+$ macrophages could be indicative of a foreign body response [30,31]. Macrophages were found nearly exclusively within the borders of the implants, evenly dispersed throughout the tissue by 2 weeks (**Figures 6A-D**). Similar to overall inflammatory infiltrate, macrophage area was approximately similar for each group at early time points, but AD scaffolds were associated with a significant decrease in total macrophage coverage compared to other groups by 4 weeks (**Figure 6E**). Based on these data, AD scaffolds are

relatively non-immunogenic, inducing lower inflammatory and stromal reactions than DD nerve grafts and even the isograft negative controls.

## 4. Discussion

While several decellularization protocols have been developed for a variety of tissues, many protocols start by lysing cells in hypotonic water, thereby dispersing antigens throughout the tissue and causing tissue swelling. Detergents, proteolytic enzymes, and/or other chemical treatments are then necessary to remove the resulting cellular debris, with added risk of damaging the tissue structure and composition [11,13,14]. To overcome these drawbacks, recent efforts have aimed to describe potentially less damaging methods of cellular removal.

Flushing with supercritical carbon dioxide followed by rapid depressurization has been used to decellularize cardiac tissue at the cost of inducing cell lysis but with the added benefit of sterilizing the end product [32]. A different method leveraged the concept of Wallerian degeneration to promote axonal dieback in peripheral nerve tissue *in vitro*, followed by extensive washing in PBS [7]. This process effectively preserved the tissue structure but required three weeks to complete and is narrowly specific to nervous tissue. Treating with latrunculin B has also been used to induce a more general process of actin depolymerization, promoting cellular detachment and removal within cardiac and muscle tissue [33,34]. Nonetheless, this method removed some beneficial components of the extracellular matrix, similar to many other protocols.

The objective of the present study was to develop a widely applicable method of decellularization without the use of damaging reagents by capitalizing on the inherent biological process of apoptosis. Apoptosis is characterized by the degradation of antigenic cellular components, cellular detachment from the extracellular matrix, and formation of small, membrane-bound apoptotic bodies [18]. These cellular fragments would theoretically be easier to remove from tissue compared to whole cells and therefore negate the need for cell lysis buffers, damaging surfactants, or extensive periods of debris clearance. Leveraging apoptosis for decellularization was first proposed by Bourgine et al. [35] and has since been shown an effective method to create *de novo* matrices from cells engineered to respond to pro-apoptotic signals [36,37]. To the authors' knowledge, induction of apoptosis has not yet been shown effective as a means to gently decellularize native tissue *ex vivo*.

We demonstrated that it is possible to induce apoptosis in *ex vivo* nerve tissue using the cytotoxic compound camptothecin. While camptothecin is primarily known to induce cell death through inhibition of topoisomerase I in dividing cells [15,38], topoisomerase-independent mechanisms have also been shown in non-dividing cells such as post-mitotic neurons [23]. *In vitro* exposure to this broad-spectrum drug induced two markers of apoptosis in nerve tissue: cleaved caspase-3 expression and DNA fragmentation ($TUNEL^+$ staining). Cleaved caspase-3 staining was identifiable both in axonal processes stained for neurofilament as well as in nonneural cells that did not express neurofilament, suggesting camptothecin was able to induce apoptosis in many of the different cell types found in peripheral nerve.

Induction of apoptosis alone was not sufficient to decellularize the tissue; however, cellular and myelin-associated proteins were easily removed using a 24 hour wash in hypertonic (4X) PBS. Washing non-treated tissue with this buffer did not observably reduce cellular protein immunoreactivity, suggesting that apoptosis was required for this wash to be effective. Additionally, washing in hypertonic saline preserved the basal lamina structure, showing nearly identical laminin staining in apoptosis decellularized (AD) nerves compared to unprocessed tissue. This result was in sharp contrast to the structural disruption found in tissue incubated in water, the first step in many other decellularization protocols. Additional studies are required to assess if this preservation in tissue structure indeed improves regenerative potential. While hypertonic saline did not significantly alter the DNA content, adding a step to treat with the nucleolytic enzyme DNase effectively achieved >95% DNA removal, a suggested benchmark for adequate decellularization [24].

During optimization of the decellularization protocol, it was found that 1 day of drug treatment prior to washing achieved the best protein and DNA removal despite an enhancement in apoptosis markers at longer times. These data suggest that the early stage of apoptosis can facilitate cell removal, but cells entering the later stages of apoptosis may start to inhibit removal. This may be explained by a process called secondary necrosis, which is the lysis of apoptotic bodies not cleared by phagocytosis *in vivo* [39]. Exposing nerve tissue to apoptotic signals for short periods may decrease secondary necrosis/cell lysis and therefore improve antigen removal.

The optimized wash strategy of hypertonic buffer followed by DNase sufficiently removed cytotoxic residuals from the apoptosis induction step. Medium conditioned with AD nerve did not significantly affect the metabolism of cultured Schwann cells. In contrast, conditioned medium from detergent decellularized (DD) nerves had the largest impact on Schwann cell metabolism, decreasing their metabolism by half. This *in vitro* effect is likely the result of incomplete washing following detergent processing since these nerve grafts are known to be tolerated *in vivo* [26]. Furthermore, the reduction in metabolic activity observed using unprocessed nerve conditioned medium might be attributed to signals released from dying cells over the conditioning period.

Ultimately, the test for effective decellularization is examining the immunogenic potential *in vivo*. Incomplete decellularization can exacerbate pro-inflammatory reactions and limit tissue reconstruction [12]. Subcutaneous implantation of AD nerves was not associated with major signs of immune rejection. In fact, AD scaffold exhibited decreased inflammatory infiltration and phagocytic macrophage coverage compared to allograft positive controls and even the isograft negative controls (equivalent to human autografts). Therefore, decellularizing nerve tissue by first inducing apoptosis prior to washing can effectively remove antigenic components to limit the resulting host inflammatory response while enhancing the structural preservation without the need for cell lysis or harsh reagents such as detergents.

Although we employed camptothecin here, the concept may be adapted to an array of endogenous biological compounds [40,41] as well as exogenous or synthetic small molecules [42–44]. The recently identified small molecule Raptinal induced apoptosis

within minutes in a variety of cells and thereby could offer significant potential to minimize the time and resources required for decellularization [43]. The current protocol only examined use of tissue immediately after harvest, although we found no indication of apoptosis in samples incubated in medium for up to two days. Therefore, it may be possible to extend the start of decellularization, and facilitate production at a larger scale, by maintaining nerves under physiological conditions after harvest.

As noted above, neuronal cell bodies reside outside of the peripheral nerve and it is therefore unclear if the axonal caspase-3 activity and subsequent removal observed here can be accurately attributed to apoptosis. Rapid Wallerian degeneration is possible yet unlikely since this would involve caspase-6 but specifically not caspase-3 [45]. It is more likely to be, if not apoptosis, a mechanism more similar to axon pruning which does involve caspase-3 activity [46]. It is also possible that eliminating resident Schwann cells (and others) via apoptosis activates corresponding, soma-independent axonal pathways. A similar process was previously described in the central nervous system following targeted ablation of oligodendrocytes [47].

## 5. Conclusions

We have developed a novel detergent-free method of decellularization that capitalizes on the natural machinery of programmed cell death, or apoptosis. Treating *ex vivo* nerve tissue with 5–10 μM cytotoxic camptothecin, an FDA-indicated small molecule for cancer therapy, induced active caspase-3 expression and DNA fragmentation in *ex vivo* nerve tissue in as little as one day. Removal of cellular proteins and DNA was then achieved using hypertonic (4X) and mildly hypotonic (0.5X) saline solutions. Replacing the hypotonic wash with DNase further enhanced DNA removal, surpassing the desired >95% removal. Camptothecin-treated nerves retained extracellular matrix components, such as collagen and glycosaminoglycans, and also exhibited tissue architecture qualitatively identical to that of native nerve. Furthermore, apoptosis decellularized grafts were non-cytotoxic to Schwann cell cultures and were immunologically tolerated in a rat subcutaneous implant model, actually achieving a lower histological score than isograft negative controls after 4 weeks. Therefore, *ex vivo* apoptosis is an effective method to generate non-immunogenic decellularized scaffolds for not only peripheral nerve, but a wide variety of tissues.

## Supplementary Material

Refer to Web version on PubMed Central for supplementary material.

## 6. Acknowledgements

The authors would like thank Dr. Elizabeth Whitley at the University of Florida for advice on the histopathological scoring system. We also want to acknowledge funding support from the National Institutes of Health (R21EB013358), the National Science Foundation (DMR 0805298), and the Craig H. Neilsen Foundation (#222456). The National Science Foundation also supported RCC via a travel grant for disseminating work in regenerative medicine research.

Funding: This work was supported by the National Institute of Health [R21EB013358]; the National Science Foundation [DMR 0805298]; and Craig Neilsen Foundation [grant #222456] 29

## 8. References


[1]. Kolewe ME, Park H, Gray C, Ye X, Langer R, Freed LE. 3D structural patterns in scalable, elastomeric scaffolds guide engineered tissue architecture. Adv Mater. 2013;25(32):4459–65. [PubMed: 23765688]

[2]. Yannas IV. Emerging rules for inducing organ regeneration. Biomaterials. 2013;34(2):321–30. [PubMed: 23092865]

[3]. Spivey EC, Khaing ZZ, Shear JB, Schmidt CE. The fundamental role of subcellular topography in peripheral nerve repair therapies. Biomaterials 2012 p. 4264–76. [PubMed: 22425024]

[4]. Hoffman-Kim D, Mitchel JA, Bellamkonda R V. Topography, Cell Response, and Nerve Regeneration. Annu Rev Biomed Eng. 2010;12(1):203–31. [PubMed: 20438370]

[5]. Boriani F, Fazio N, Fotia C, Savarino L, Nicoli Aldini N, Martini L, Zini N, Bernardini M, Baldini N. A novel technique for decellularization of allogenic nerves and in vivo study of their use for peripheral nerve reconstruction. J Biomed Mater Res - Part A. 2017;105(8):2228–40.

[6]. Sridharan R, Reilly RB, Buckley CT. Decellularized grafts with axially aligned channels for peripheral nerve regeneration. J Mech Behav Biomed Mater. 2015;41:124–35. [PubMed: 25460409]

[7]. Vasudevan S, Huang J, Botterman B, Matloub HS, Keefer E, Cheng J. Detergent-free decellularized nerve grafts for long-gap peripheral nerve reconstruction. Plastic and Reconstructive Surgery. 2014;e201. [PubMed: 25426384]

[8]. Hudson TW, Liu SY, Schmidt CE. Engineering an improved acellular nerve graft via optimized chemical processing. Tissue Eng. 2004;10(9–10):1346–58. [PubMed: 15588395]

[9]. Sondell M, Lundborg G, Kanje M. Regeneration of the rat sciatic nerve into allografts made acellular through chemical extraction. Brain Res. 1998;795(1–2):44–54. [PubMed: 9622591]

[10]. Gilbert TW, Sellaro TL, Badylak SF. Decellularization of tissues and organs. Vol. 27, Biomaterials. 2006 p. 3675–83. [PubMed: 16519932]

[11]. Crapo PM, Gilbert TW, Badylak SF. An overview of tissue and whole organ decellularization processes. Biomaterials NIH Public Access; 4, 2011 p. 3233–43.

[12]. Keane TJ, Londono R, Turner NJ, Badylak SF. Consequences of ineffective decellularization of biologic scaffolds on the host response. Biomaterials. 2012;33(6):1771–81. [PubMed: 22137126]

[13]. Guyette JP, Gilpin SE, Charest JM, Tapias LF, Ren X, Ott HC. Perfusion decellularization of whole organs. Nat Protoc. 2014;9(6):1451–68. [PubMed: 24874812]

[14]. Faulk DM, Carruthers CA, Warner HJ, Kramer CR, Reing JE, Zhang L, D'Amore A, Badylak SF. The effect of detergents on the basement membrane complex of a biologic scaffold material. Acta Biomater. 2014;10(1):183–93. [PubMed: 24055455]

[15]. Katyal S, Lee Y, Nitiss KC, Downing SM, Li Y, Shimada M, Zhao J, Russell HR, Petrini JHJ, Nitiss JL, McKinnon PJ. Aberrant topoisomerase-1 DNA lesions are pathogenic in neurodegenerative genome instability syndromes. Nat Neurosci. 2014;17(6):813–21. [PubMed: 24793032]

[16]. Vaseva A V, Marchenko ND, Ji K, Tsirka SE, Holzmann S, Moll UM. P53 opens the mitochondrial permeability transition pore to trigger necrosis. Cell. 2012;149(7):1536–48. [PubMed: 22726440]

[17]. Yeung J, Ha TJ, Swanson DJ, Goldowitz D. A Novel and Multivalent Role of Pax6 in Cerebellar Development. J Neurosci. 2016;36(35):9057–69. [PubMed: 27581449]

[18]. Elmore S Apoptosis: A Review of Programmed Cell Death. Toxicologic Pathology 6, 2007 p. 495–516. [PubMed: 17562483]

[19]. Siu PM, Tam EW, Teng BT, Pei XM, Ng JW, Benzie IF, Mak AF. Muscle apoptosis is induced in pressure-induced deep tissue injury. J Appl Physiol. 2009;107(4):1266–75. [PubMed: 19644027]

[20]. Wang MO, Etheridge JM, Thompson JA, Vorwald CE, Dean D, Fisher JP. Evaluation of the in vitro cytotoxicity of cross-linked biomaterials. Biomacromolecules. 2013;14(5):1321–9. [PubMed: 23627804]

[21]. O'Neill JD, Freytes DO, Anandappa AJ, Oliver JA, Vunjak-Novakovic GV. The regulation of growth and metabolism of kidney stem cells with regional specificity using extracellular matrix derived from kidney. Biomaterials. 2013;34(38):9830–41. [PubMed: 24074840]

[22]. Mukhatyar V, Pai B, Clements I, Srinivasan A, Huber R, Mehta A, Mukhopadaya S, Rudra S, Patel G, Karumbaiah L, Bellamkonda R. Molecular sequelae of topographically guided peripheral nerve repair. Ann Biomed Eng. 2014;42(7):1436–55. [PubMed: 24356852]

[23]. Morris EJ, Geller HM. Induction of neuronal apoptosis by camptothecin, an inhibitor of DNA topoisomerase-I: Evidence for cell cycle-independent toxicity. J Cell Biol. 1996;134(3):757–70. [PubMed: 8707853]

[24]. Caralt M, Uzarski JS, Iacob S, Obergfell KP, Berg N, Bijonowski BM, Kiefer KM, Ward HH, Wandinger-Ness A, Miller WM, Zhang ZJ, Abecassis MM, Wertheim JA. Optimization and critical evaluation of decellularization strategies to develop renal extracellular matrix scaffolds as biological templates for organ engineering and transplantation. Am J Transplant. 2015;15(1):64–75. [PubMed: 25403742]

[25]. Seif-Naraghi SB, Horn D, Schup-Magoffin PJ, Christman KL. Injectable extracellular matrix derived hydrogel provides a platform for enhanced retention and delivery of a heparin-binding growth factor. Acta Biomater. 2012;8(10):3695–703. [PubMed: 22750737]

[26]. Hudson TW, Zawko S, Deister C, Lundy S, Hu CY, Lee K, Schmidt CE. Optimized acellular nerve graft is immunologically tolerated and supports regeneration. Tissue Eng. 2004;10(11–12):1641–51. [PubMed: 15684673]

[27]. Harley BA, Spilker MH, Wu JW, Asano K, Hsu HP, Spector M, Yannas IV. Optimal Degradation Rate for Collagen Chambers Used for Regeneration of Peripheral Nerves over Long Gaps In: Cells Tissues Organs. 2004 p. 153–65.

[28]. Nectow AR, Marra KG, Kaplan DL. Biomaterials for the Development of Peripheral Nerve Guidance Conduits. Tissue Eng Part B Rev. 2012;18(1):40–50. [PubMed: 21812591]

[29]. Donnelly DJ, Gensel JC, Ankeny DP, van Rooijen N, Popovich PG. An efficient and reproducible method for quantifying macrophages in different experimental models of central nervous system pathology. J Neurosci Methods. 2009;181(1):36–44. [PubMed: 19393692]

[30]. Gaudet AD, Popovich PG, Ramer MS. Wallerian degeneration: Gaining perspective on inflammatory events after peripheral nerve injury. Vol. 8, Journal of Neuroinflammation. 2011.

[31]. Cronce MJ, Faulknor RA, Pomerantseva I, Liu XH, Goldman SM, Ekwueme EC, Mwizerwa O, Neville CM, Sundback CA. In vivo response to decellularized mesothelium scaffolds. J Biomed Mater Res - Part B Appl Biomater. 2018;106(2):716–25. [PubMed: 28323397]

[32]. Guler S, Aslan B, Hosseinian P, Aydin HM. Supercritical Carbon Dioxide-Assisted Decellularization of Aorta and Cornea. Tissue Eng Part C Methods. 2017;23(9):540–7. [PubMed: 28726559]

[33]. Assmann A, Struß M, Schiffer F, Heidelberg F, Munakata H, Timchenko E V., Timchenko PE, Kaufmann T, Huynh K, Sugimura Y, Leidl Q, Pinto A, Stoldt VR, Lichtenberg A, Akhyari P. Improvement of the in vivo cellular repopulation of decellularized cardiovascular tissues by a detergent-free, non-proteolytic, actin-disassembling regimen. J Tissue Eng Regen Med. 2017;11(12):3530–43. [PubMed: 28078820]

[34]. Gillies AR, Smith LR, Lieber RL, Varghese S. Method for Decellularizing Skeletal Muscle Without Detergents or Proteolytic Enzymes. Tissue Eng Part C Methods. 2011;17(4):383–9. [PubMed: 20973753]

[35]. Bourgine PE, Pippenger BE, Todorov A, Tchang L, Martin I. Tissue decellularization by activation of programmed cell death. Biomaterials. 2013;34(26):6099–108. [PubMed: 23721795]

[36]. Bourgine PE, Scotti C, Pigeot S, Tchang LA, Todorov A, Martin I. Osteoinductivity of engineered cartilaginous templates devitalized by inducible apoptosis. Proc Natl Acad Sci. 2014;111(49):17426–31. [PubMed: 25422415]

[37]. Bourgine PE, Gaudiello E, Pippenger B, Jaquiery C, Klein T, Pigeot S, Todorov A, Feliciano S, Banfi A, Martin I. Engineered Extracellular Matrices as Biomaterials of Tunable Composition and Function. Adv Funct Mater. 2017;27(7).

[38]. Traganos F, Seiter K, Feldman E, Halicka HD, Darzynkiewicz Z. Induction of apoptosis by camptothecin and topotecan In: Annals of the New York Academy of Sciences. 1996 p. 101–10.

[39]. Silva MT. Secondary necrosis: The natural outcome of the complete apoptotic program. FEBS Letters 2010 p. 4491–9. [PubMed: 20974143]

[40]. Czubowicz K, Strosznajder R. Ceramide in the Molecular Mechanisms of Neuronal Cell Death. The Role of Sphingosine-1-Phosphate. Mol Neurobiol. 2014;50(1):26–37. [PubMed: 24420784]

[41]. Wood LB, Winslow AR, Proctor EA, McGuone D, Mordes DA, Frosch MP, Hyman BT, Lauffenburger DA, Haigis KM. Identification of neurotoxic cytokines by profiling Alzheimer's disease tissues and neuron culture viability screening. Sci Rep. 2015;5.

[42]. Xin M, Li R, Xie M, Park D, Owonikoko TK, Sica GL, Corsino PE, Zhou J, Ding C, White MA, Magis AT, Ramalingam SS, Curran WJ, Khuri FR, Deng X. Small-molecule Bax agonists for cancer therapy. Nat Commun. 2014;5.

[43]. Palchaudhuri R, Lambrecht MJ, Botham RC, Partlow KC, van Ham TJ, Putt KS, Nguyen LT, Kim S-HH, Peterson RT, Fan TM, Hergenrother PJ. A Small Molecule that Induces Intrinsic Pathway Apoptosis with Unparalleled Speed. Cell Rep. 2015;13(9):2027–36. [PubMed: 26655912]

[44]. Pommier Y Topoisomerase I inhibitors: Camptothecins and beyond In: Nature Reviews Cancer. 2006 p. 789–802.

[45]. King AE, Southam KA, Dittmann J, Vickers JC. Excitotoxin-induced caspase-3 activation and microtubule disintegration in axons is inhibited by taxol. Acta Neuropathol Commun. 2013;1(1): 59. [PubMed: 24252213]

[46]. Cusack CL, Swahari V, Hampton Henley W, Michael Ramsey J, Deshmukh M. Distinct pathways mediate axon degeneration during apoptosis and axon-specific pruning. Nat Commun. 2013;4.

[47]. Ghosh A, Manrique-Hoyos N, Voigt A, Schulz JB, Kreutzfeldt M, Merkler D, Simons M. Targeted ablation of oligodendrocytes triggers axonal damage. PLoS One. 2011;6(7).

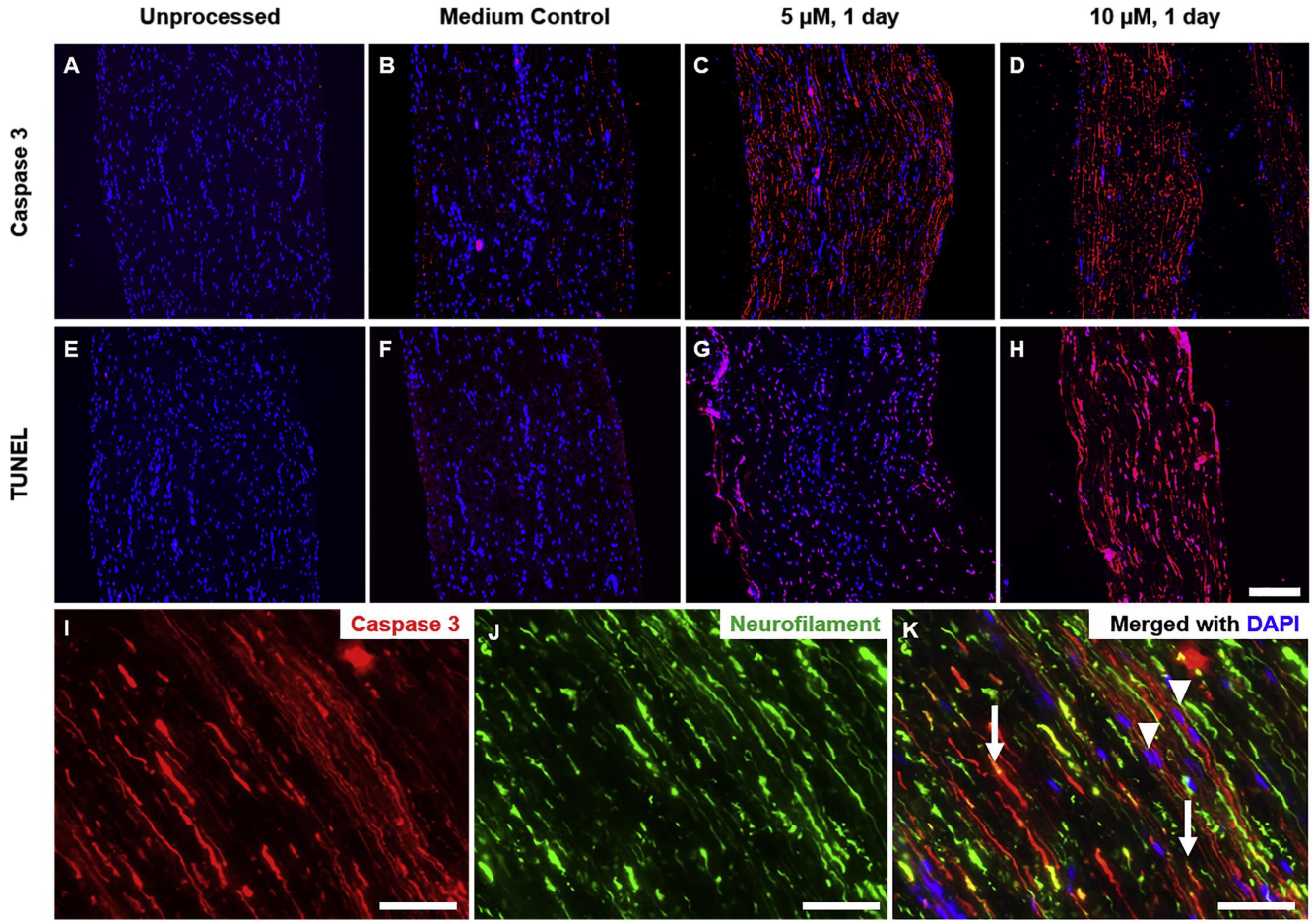


**Figure 1:**

Camptothecin induces apoptosis in ex vivo nerve tissue. Fluorescence micrographs of tissue labeled using anti-active caspase 3 (A-D) and TUNEL (E-H) in red. Staining is shown for untreated fresh nerves (A, E) and nerves treated with camptothecin for one day in vitro at 0 μM (B, F), 5 μM (C, G), and 10 μM (D, H). Nuclei are counterstained with DAPI (blue). Scale bar is 200 μm. Processing and staining was repeated at least three times per group. (I-K) Images from a longitudinal section of a drug-treated nerve, imaged at 20X and enlarged to show detail. Arrows indicate colocalization of cleaved caspase-3 and neurofilament, suggestive of axonal staining. Arrowheads indicate cleaved caspase-3 staining associated with a nucleus but not with neurofilament, suggesting non-neuronal staining such as fibroblasts or Schwann cells. Scale bar is 50 μm.

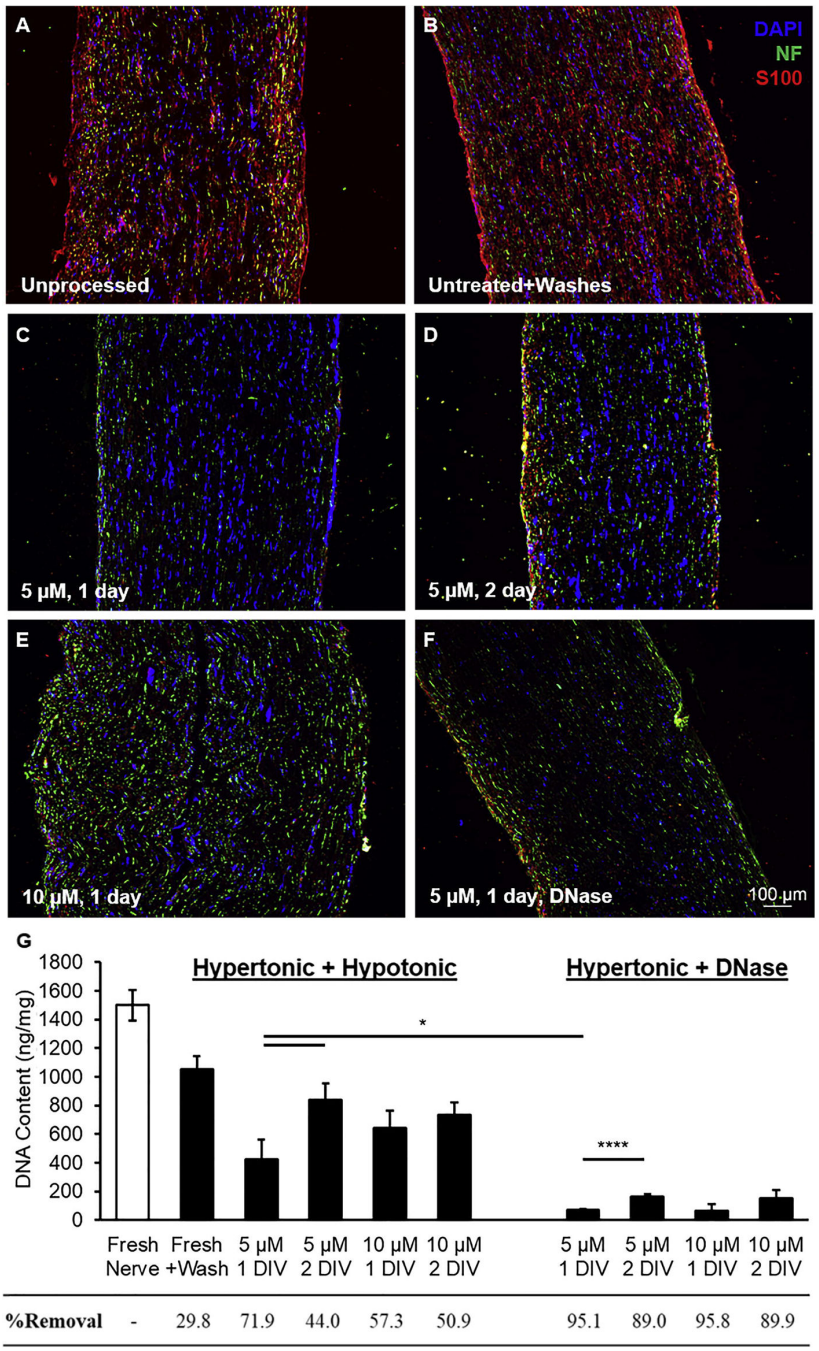


**Figure 2:**

Apoptosis induction facilitates decellularization using nonisotonic buffers. Representative images of immunofluorescent staining for neurofilament (NF, neurons, green) and S100 (Schwann cells, red) in (A) unprocessed fresh nerve, (B) fresh nerve + hypertonic/ hypotonic washes, and (C-F) nerves washed in buffer(s) after treating with camptothecin at 5 μM for 1 day (C and F), 5 μM for 2 days (D), 10 μM for 1 day, or 10 μM for 2 days. The tissues in (C-E) were washed using hypertonic/ hypotonic buffers (24 and 18 hours, respectively), while F was washed only with hypertonic buffer followed by DNase treatment. Nuclei are shown in

blue (DAPI). Processing and staining was repeated at least three times per group. (G) DNA quantification for all groups of unprocessed and processed nerve tissue. Treatment with camptothecin was necessary for cellular removal via hypertonic/ hypotonic buffers, with 5 M for 1 day performing best. Effective DNA removal (>95%) required treatment with DNase over hypotonic buffers. All data were significantly different than unprocessed nerve ($p<0.05$ or less), and all data were significantly different than untreated nerve+washes ($p<0.05$ or less) except 5 μM 2 day with the hypertonic/hypotonic washes ($p>0.1$). Error bars represent standard error with n=5 per group. *$p<0.05$ and ****$p<0.001$.

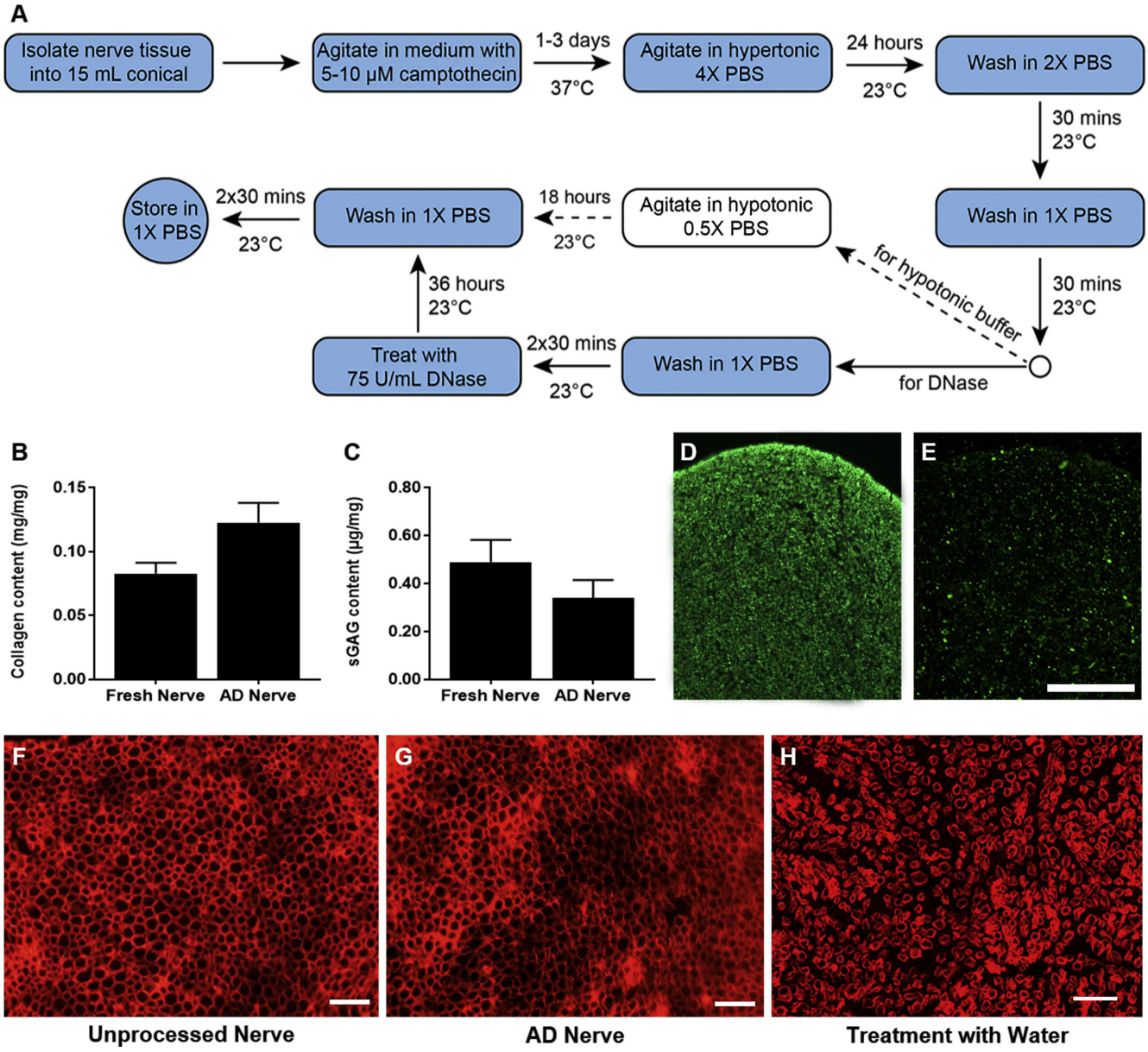


**Figure 3:**

Apoptosis decellularization preserves desirable matrix components and structure but not myelin proteins. (A) Flow diagram of the generalize process for apoptosis decellularization. Dashed arrows indicate steps that were excluded from the final process for nerve tissue. (B) Quantification of collagen content before and after apoptosis decellularization (n=4). (C) Quantification of sulfated GAGs before and after apoptosis decellularization (AD) (n=5). Neither quantification revealed a significant difference. Immunoreactivity for myelin basic protein was assessed for unprocessed nerve (D) and apoptosis decellularized nerve (E). (F-H) Fluorescence micrographs of laminin staining in fresh nerve (F), apoptosis decellularized nerve (G), and fresh nerve processed with water for cell lysis (H). Processing and staining was repeated at least three times per group. Scale bars represents 50 μm. No significant difference was found in B or C.

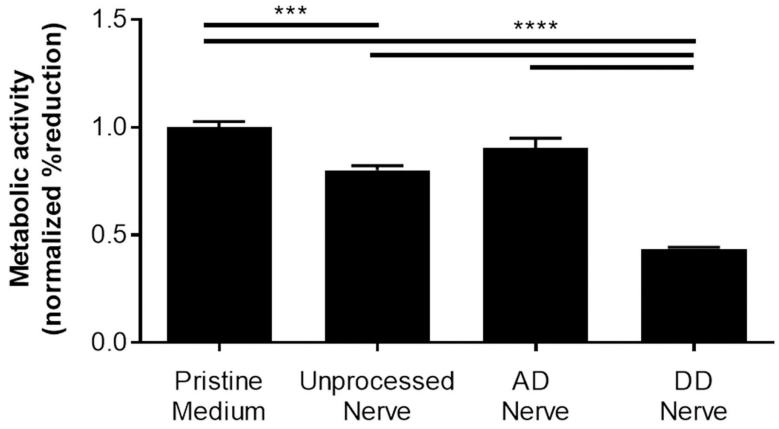


**Figure 4:**

Apoptosis decellularized nerve grafts are non-cytotoxic in vitro. The metabolic activity of Schwann cells was measured using reduction of alamarBlue following culture in media conditioned with either unprocessed, apoptosis decellularized (AD), or detergent decellularized (DD) nerves. Medium conditioned without tissue (pristine) was used as a control. Error bars represent standard error (n=5). ***p<0.001 ****p<0.0001.

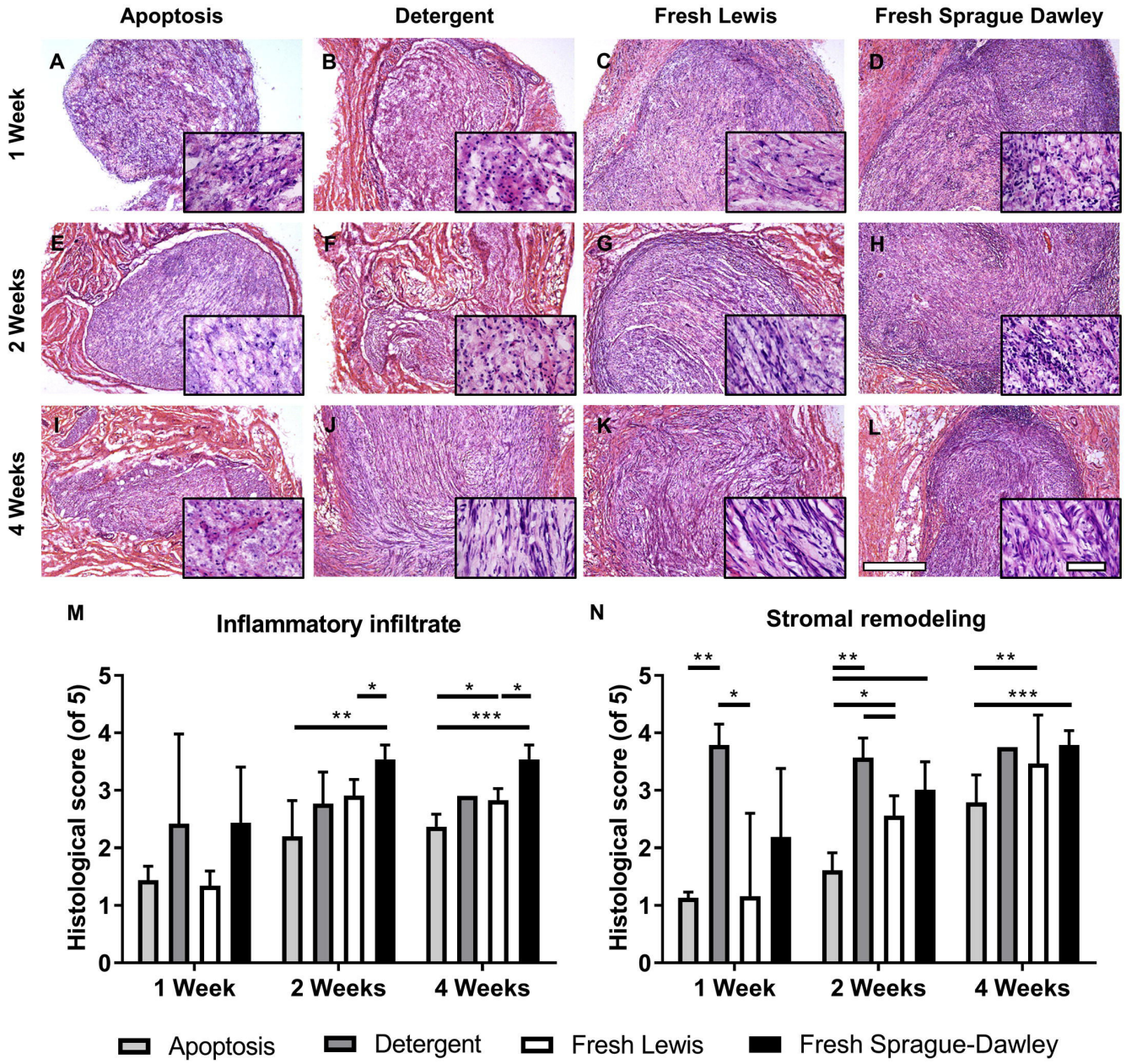


**Figure 5:**

Apoptosis-decellularized nerves are immunologically tolerated, with decreased inflammatory infiltrate and stromal remodeling compared to isograft by 4 weeks. Tissue from one of four groups (apoptosis decellularized, detergent decellularized, or fresh Lewis and Sprague-Dawley controls) was implanted subcutaneously for 1–4 weeks (n=4). (A-L) Brightfield H&E images for an example explant per group showing areas of infiltrates and stromal changes at weeks 1, 2, and 4. Images are at 5x with 40x inset images to show detail within the implant. Scale bars represent 500 μm for 5X images and 50 μm for 40X images. (M) Quantitative histological scoring of inflammatory infiltrates at the center at 1, 2, and 4 weeks. (N) Quantitative scoring of stromal cells at the center at 1, 2, and 4 weeks. Error bars

represent standard error with n=4 except detergent decellularized at 4 weeks (n=1). *p<0.05 **p<0.01 ***p<0.001.

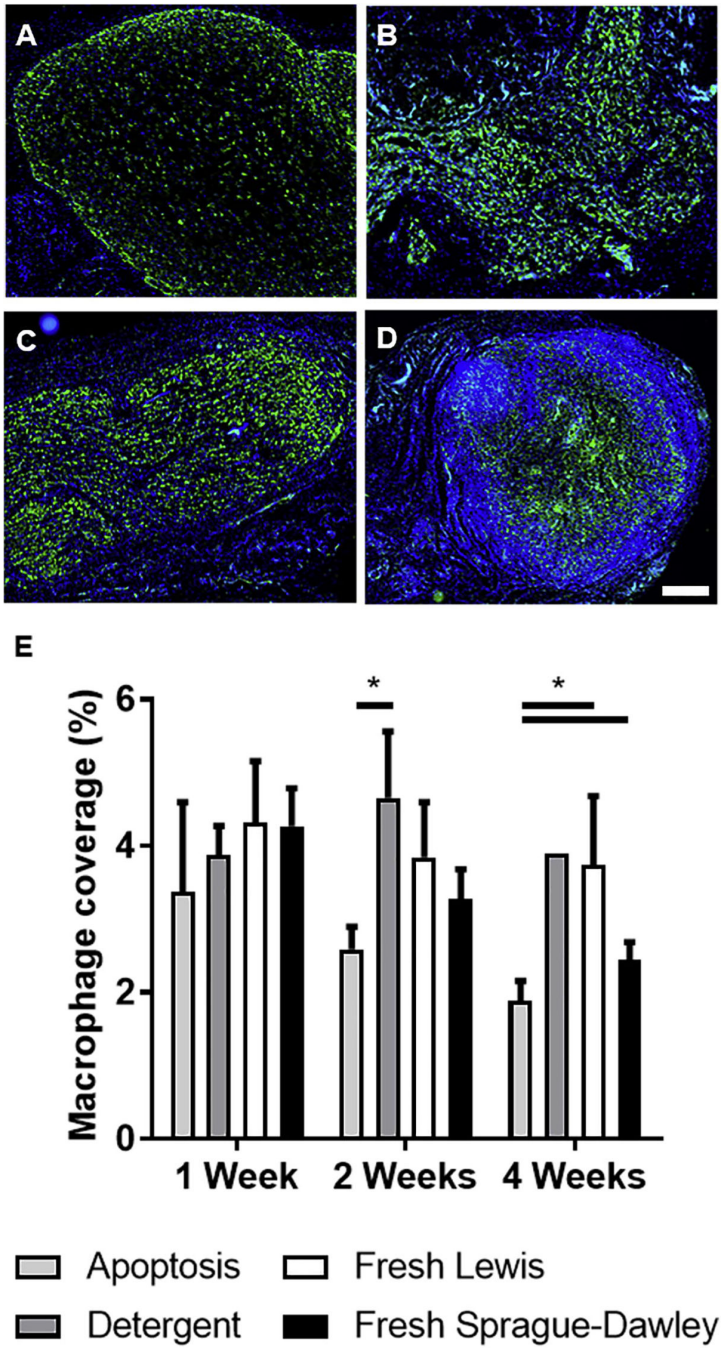


**Figure 6:**

Apoptosis decellularized grafts show decreased macrophage infiltration. (A-D) Representative images of explanted 2 week tissue immuno-fluorescently stained for CD68 (pan-macrophage, green) in (A) AD nerve, (B) DD nerve, (C) unprocessed Lewis nerve, and (D) unprocessed Sprague-Dawley nerve. Nuclei were counterstained with DAPI (blue). Scale bar is 500 μm. (E) Macrophage quantification as a percent of area coverage. Error bars represent standard error with n=4 except detergent decellularized at 4 weeks (n=1). *$p<0.05$.